

METHODOLOGY AND ALGORITHM FOR 3D RECONSTRUCTION OF THE GEOMETRY OF VESSELS FROM BIPLANE ANGIOGRAPHIC VIEWS

T. Manos⁽¹⁾, M. Pilou⁽¹⁾, D.P. Sokolis⁽²⁾, C.A. Dimitriou⁽²⁾, J.D. Kakisis⁽³⁾,
P.E. Karayannacos⁽²⁾, S. Tsangaris⁽¹⁾

⁽¹⁾ Laboratory of Biofluid-Mechanics and Biomedical Engineering,
National Technical University of Athens, Athens, Greece

⁽²⁾ Centre of Experimental Surgery, Foundation of Biomedical Research,
Academy of Athens, Athens, Greece

⁽³⁾ Vascular Unit, 3rd Department of Surgery, University of Athens
School of Medicine, Attikon University Hospital, Athens, Greece

Key words: biplane angiography, arteriovenous anastomosis, 3D geometry, algorithm, parametric natural spline

Abstract. *A methodology and the respective algorithm was developed for (1) the determination of the 3D geometry of blood vessel central lines from biplane angiographic views and (2) the drawing of circular cross-sections at selected positions for the approximation of vessel lumen. Our methodology required preceding knowledge of the position vectors of a pair of points on the plane views, for calculation of the rotation matrix and translation vector that relate the two coordinate systems. For identification of the pair of points on the two views, the epipolar line technique was used, while the central line was reconstructed via a parametric natural spline.*

1. INTRODUCTION

It is known that the majority of PTFE arteriovenous grafts are blocked within 18 months post-implantation, due to intimal hyperplasia at the venous anastomosis.

Various factors have been incriminated for the development of intimal hyperplasia, the most important being mechanical injury of the vessel wall, compliance mismatch between graft and vessel and disturbance of haemodynamic conditions in the region of anastomosis.

Research regarding the role of haemodynamics in the development of intimal hyperplasia at the venous anastomosis of arteriovenous grafts focuses on the precise calculation of blood flow variables, i.e. determination of the blood velocity field, the distribution of wall shear stresses and turbulence, etc. The problem is solved by utilizing methods of computational fluid dynamics, which require knowledge of the vessel geometry.

One of the conventional ways of vascular imaging is biplane angiography, amounting to projection of the vessel onto two different planes using a radiation source. From those two projections, characteristic points are defined by manual selection or automatically with the use of image processing. These points are then taken as inputs in a custom-made algorithm, which extracts the 3D vessel geometry. This data together with the boundary condition information can be employed in a computational fluid dynamics algorithm that will provide the solution of the flow field.

A methodology, which is based on the Metz – Fencil technique (Metz & Fencil^[1]), and the corresponding algorithm for determination of the 3D geometry of vessels from biplane angiography are described in the present study. We specify the problem to be solved and introduce the theoretical background for the various stages of reconstruction. Subsequently, the algorithm is tested on a theoretical model of known geometry and the achieved reconstruction is shown.

2. DEFINITION OF THE PROBLEM AND METHOD OF SOLUTION

The problem dealt with in the present work is the determination of 3D vessel geometry from their projections, obtained by biplane angiography, where the relation that connects the two systems of coordinates is considered unknown. The theory is based on the Metz – Fencil^[1] technique and its further development^[2, 3, 4, 5].

2.1. Geometry of the biplane imaging system

A schematic diagram of a biplane system is shown in Figure 1. The transformation relating the two 3D coordinate systems, $S1xyz$ and $S2x'y'z'$, which are defined for each single-plane system, can be expressed as

$$\begin{bmatrix} x_i' \\ y_i' \\ z_i' \end{bmatrix} = \mathbf{R} \begin{bmatrix} x_i \\ y_i \\ z_i \end{bmatrix} - \mathbf{t} \quad (1)$$

where

$$\mathbf{R} = \begin{bmatrix} r_{11} & r_{12} & r_{13} \\ r_{21} & r_{22} & r_{23} \\ r_{31} & r_{32} & r_{33} \end{bmatrix} \quad (2)$$

is the rigid rotation matrix relating the xyz to the $x'y'z'$ axes and

$$\mathbf{t} = [t_x \quad t_y \quad t_z]^T \quad (3)$$

the vector describing the 3D translation from the origin of the xyz to that of the $x'y'z'$ system, i.e. the distance between the two focal spots SIS2.

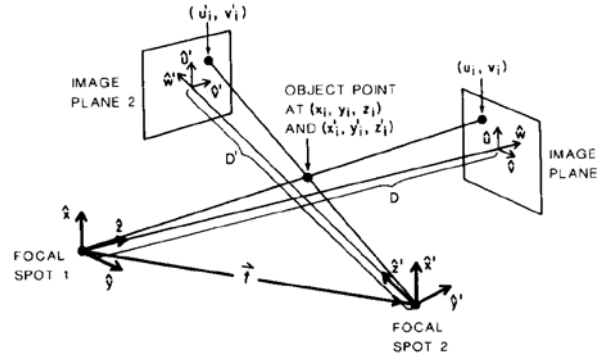


Figure 1. Schematic example of the coordinate systems for biplane projection views with arbitrary relative orientation [1].

When this imaging system is used to obtain the image of an object, which consists of a number of identifiable points, the image coordinates (u_i, v_i) for the projection of the i th point, (x_i, y_i, z_i) , are related to the 3D position of that point by

$$u_i = D \frac{x_i}{z_i}, \quad v_i = D \frac{y_i}{z_i} \quad (4)$$

where D is the source to image plane distance (SID) in the $S1xyz$ system. Dimensionless coordinates of the (x_i, y_i, z_i) point are also defined by

$$\xi_i \equiv u_i / D = x_i / z_i, \quad \eta_i \equiv v_i / D = y_i / z_i \quad (5)$$

Analogous equations are valid for the $S2x'y'z'$ system. Via these equations, \mathbf{R} and \mathbf{t} , i.e. the imaging geometry, as well as the 3D positions of the projected objects can be estimated.

Simplification for the problem under review

Purpose of this method is to facilitate the reconstruction of the 3D geometry of blood vessels. The data are obtained in experiments, where the projections are acquired by a specific portable C-arm, the BV Libra (Philips Medical Systems, P.M.G Surgery, The Netherlands), in a specific way that allows simplification of the algorithm.

During the experiments, the C-arm was positioned vertically to the longitudinal axis of the surgical table and all the translations and rotations carried on the same plane, as seen in Figure 2(a). As a result, the rotation and shift of the C-arm, and therefore also the turn and shift of the coordinate system from the first point of focus to the second, are realised exclusively on the $x-z$ plane, while the SID of projection, equal to 995 mm (Figure 2(b)), is the same in both, i.e. $D = D'$, because the dimensions of the C-arm are fixed. Consequently, both the rotation matrix and translation vector are simplified considerably

$$\begin{aligned} r_{11} &= \hat{x}'\hat{x} = \cos \vartheta, & r_{12} &= \hat{x}'\hat{y} = 0, & r_{13} &= \hat{x}'\hat{z} = \cos(\pi/2 - \vartheta) = \sin \vartheta \\ r_{21} &= \hat{y}'\hat{x} = 0, & r_{22} &= \hat{y}'\hat{y} = 1, & r_{23} &= \hat{y}'\hat{z} = 0 \\ r_{31} &= \hat{z}'\hat{x} = \cos(\pi/2 + \vartheta) = -\sin \vartheta, & r_{32} &= \hat{z}'\hat{y} = 0, & r_{33} &= \hat{z}'\hat{z} = \cos \vartheta \end{aligned} \quad (6)$$

and

$$t_x = R \sin \vartheta, \quad t_y = 0, \quad t_z = a + R(1 - \cos \vartheta) \quad (7)$$

where $R = D/2$, ϑ is the angle of rotation and a the vertical shift of the C-arm, Figure 3.

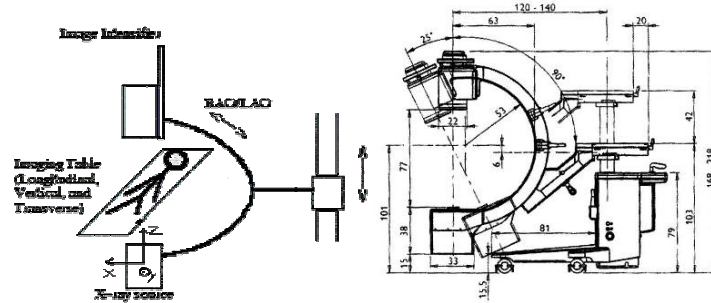


Figure 2. (a) Schematic representation of the system of angiographic imaging. Arrows indicate the executed movements during the experiments. (b) Side view of the portable C-arm (BV Libra, PHILIPS Medical Systems), displaying the characteristic dimensions.

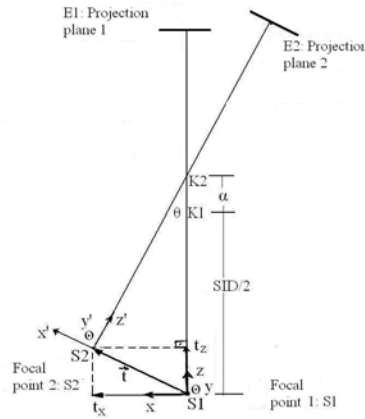


Figure 3. Systems of coordinates and the vertical shift of C-arm.

Determination of R and t

For the problem under examination, the angle of rotation and the vertical shift of the C-arm are not known in advance; these are determined via the obtained projections. Equation (1), using relations (5), (6) and (7), is written as

$$\begin{bmatrix} \xi_i \\ \eta_i \\ 1 \end{bmatrix} = \begin{pmatrix} 1 \\ \cdot \\ \cdot \end{pmatrix} \begin{bmatrix} \cos \vartheta & 0 & \sin \vartheta \\ 0 & 1 & 0 \\ -\sin \vartheta & 0 & \cos \vartheta \end{bmatrix} \begin{bmatrix} x_i - R \sin \vartheta \\ y_i \\ z_i - (a + R) + R \cos \vartheta \end{bmatrix} \quad (8)$$

Writing this matrix equation as three scalar equations, solving the third for z_i' and replacing it into the other two scalar equations, we obtain

$$\begin{cases} [(\xi_i' - \xi_i) \cos \vartheta - (\xi_i' \xi_i + 1) \sin \vartheta] z_i - (\xi_i' \cos \vartheta - \sin \vartheta)(a + R) + \xi_i' R = 0 \\ (\eta_i' \cos \vartheta - \eta_i' \xi_i \sin \vartheta - \eta_i) z_i - \eta_i' \cos \vartheta (a + R) + \eta_i' R = 0 \end{cases} \quad (9)$$

The corresponding equations for a second object point (x_j, y_j, z_j) are

$$\begin{cases} [(\xi_j' - \xi_j) \cos \vartheta - (\xi_j' \xi_j + 1) \sin \vartheta] z_j - (\xi_j' \cos \vartheta - \sin \vartheta)(a + R) + \xi_j' R = 0 \\ (\eta_j' \cos \vartheta - \eta_j' \xi_j \sin \vartheta - \eta_j) z_j - \eta_j' \cos \vartheta (a + R) + \eta_j' R = 0 \end{cases} \quad (10)$$

Equations (9) and (10) form a non-linear system of four equations with four unknowns, a , θ and z_i , z_j , which is solved using the Newton method for non-linear systems.

Consequently, the image coordinates of two object points should be recognised beforehand in both projections, so as to determine the image geometry.

2.2. Determination of the 3D coordinates of an object point

Recognition of corresponding points: epipolar line technique

Recognition of the corresponding points in the two angiographic views is done using the epipolar line technique. The line that connects a given point of the object's central line in the first view and the corresponding focal spot is projected to the second view. The point that the projected line cuts the object's central line in the second view corresponds to the given point on the first projection (Figure 4).

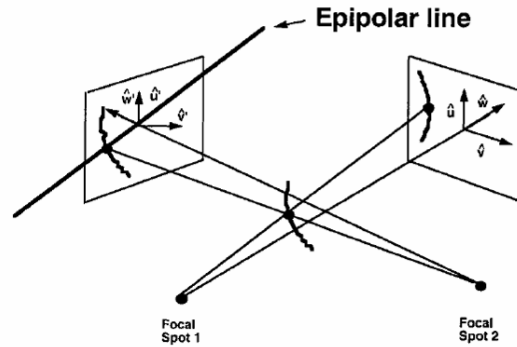


Figure 4. Schematic example of the epipolar line technique.

3D coordinates of object point

Having recognized a pair of corresponding points, $P1(u_p, v_p, D)$ and $P2(u'_p, v'_p, D)$ on the two projections using the epipolar line technique, the 3D coordinates of the object's point $P(x_p, y_p, z_p)$, which they depict, can be found with respect to the $S1xyz$ system of coordinates, with the use of equations (5)-(8).

2.3. Parametric natural spline

Interpolation via a parametric natural spline is applied in order to reconstruct the central line of vessels from the points that have been selected. Let $f(x)$ be a function defined in the $[\alpha, \beta]$ interval and $\alpha = x_1 < x_2 < \dots < x_n = \beta$ a set of points. A third degree spline S is used that interpolates function $f(x)$. In every subinterval, the spline is given by the equation:

$$S_i(x) = a_i + b_i(x - x_i) + c_i(x - x_i)^2 + d_i(x - x_i)^3, \quad i = 1, 2, \dots, n-1 \quad (11)$$

A parametric spline is the composition of two different splines, as described above. In this case, the length of arc s that connects two points is used as parameter. This way, in order to approximate function $f(x)$ we create two different splines, one that relates the variable x with parameter s , and a second that relates variable $f(x)$ with parameter s ; as a result, two interpolation functions are defined: $S(x)$ and $S(f(x))$. Accordingly, given the value of arc length s for a random point in the interval $[\alpha, \beta]$, x and $f(x)$ that correspond to this point can be defined independently of each other, obtaining the interpolation of function $f(x)$.

The parametric spline is superior compared to the simple one, because parameter s "conceives" much better sharp shifts exhibited by function $f(x)$, since it expresses the distance between the two points. Another very important advantage of the parametric spline is that points not constituting a function may be interpolated; for example, we can reconstruct a circle, something not possible with a typical spline.

2.4. Creation of circular cross-sections

After the reconstruction of the vessel's central line, circular cross-sections are added in selected positions of the central line in an attempt to partially reconstruct the vessel pipe. Every circular cross-section has as a centre a point of the central line and is perpendicular to the central line at this site.

2.5. Algorithm

The described methodology was used to develop an algorithm for reconstruction of the centre lines of objects from two angiographic projections, without prior knowledge of the imaging system geometry. This algorithm was implemented in MATLAB and its basic steps are shown in chart 1.

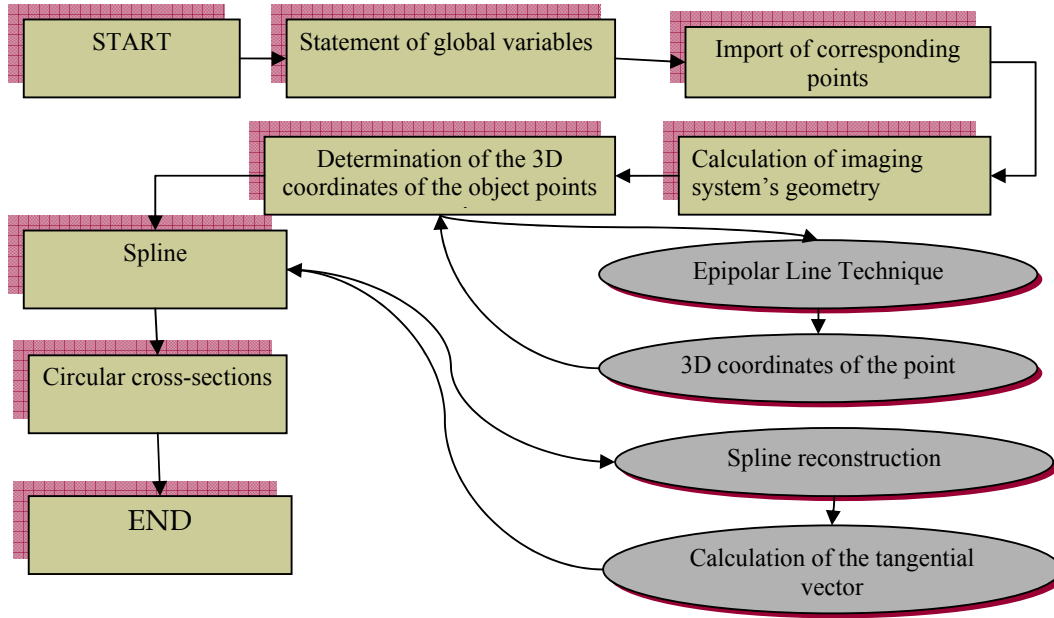


Chart 1. Schematic flow chart of the algorithm.

3. RESULTS AND DISCUSSION

3.1. Investigation of the developed methodology

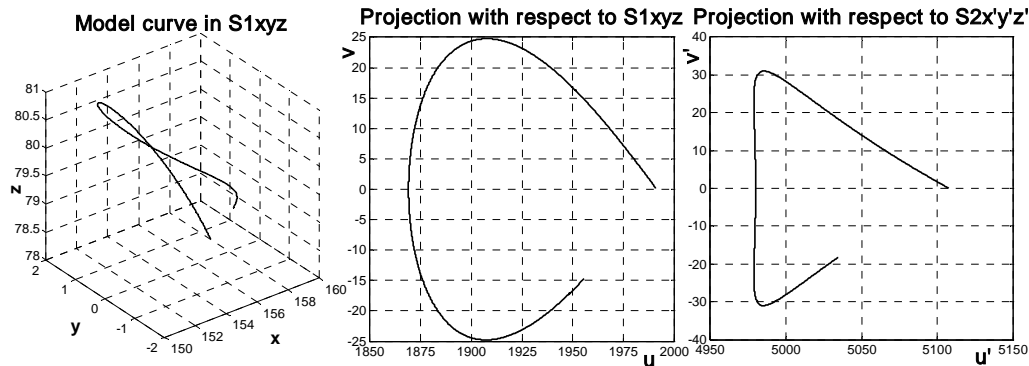


Figure 5. The 3D curve used for investigation of the method and its two projections.

For investigating the power of the proposed method in connection with the number and quality of the spline control points, the 3D curve of Figure 5 was used. The same figure also depicts the projections of the curve, obtained with an angle of rotation $\theta = -20^\circ$ and a vertical shift of the C-arm by $a = 100$ mm.

In the following Figure 6, the reconstruction of the model curve is presented with respect to the number of selected control points for the parametric spline.

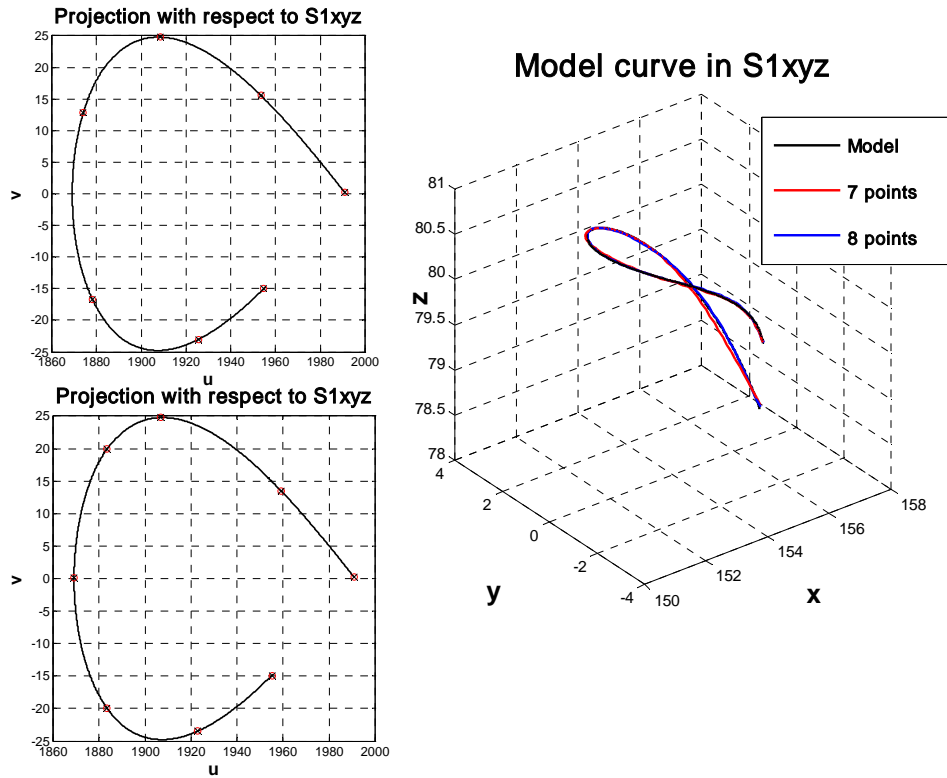


Figure 6. Reconstruction with 7 and 8 spline control points. The reconstruction does not improve considerably.

By the preceded investigation, it is shown that both the number and precision of points are critical factors in defining the subject's central line from its projections via a parametric spline. Another equally important conclusion is that for the reconstruction of a curve there is an upper limit for the number of required control points, above which the precision of reconstruction does not improve significantly. Furthermore, it should be noted that the quality of selected control points, i.e. their position, is also very important. More points and closer to each other should be selected at sites of high curvature, while lesser are needed for linear or almost linear segments. For the used model curve of Figure 6, it appears that no more than seven carefully selected control points are required to achieve a very precise reconstruction.

3.2. Theoretical application

The developed algorithm is used for reconstruction of the central line and creation of circular cross-sections of an object of known geometry from its two projections. The geometry of the model is analogous to a jugular venous anastomosis of an arteriovenous graft. The 3D geometry of the model and its two projections are shown in Figure 7. The second projection results from the turn by $\theta = -20^\circ$ and vertical shift by $a = 100$ mm of the S1xyz coordinate system.

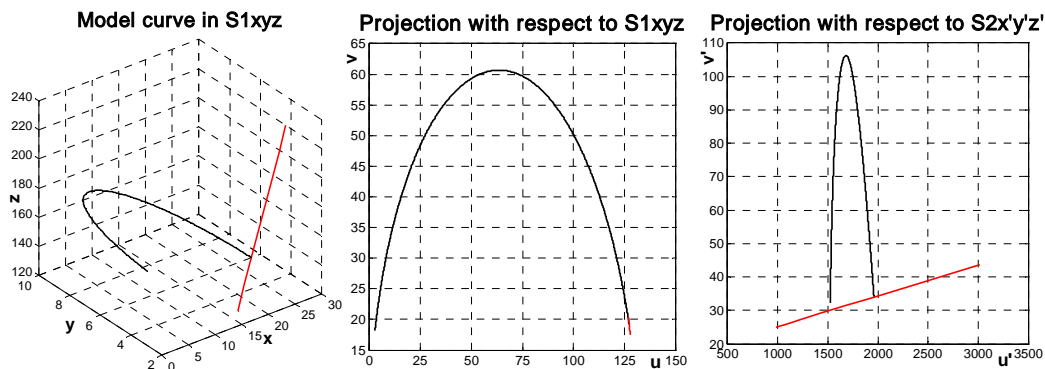


Figure 7. Model geometry of the venous anastomosis and its projections.

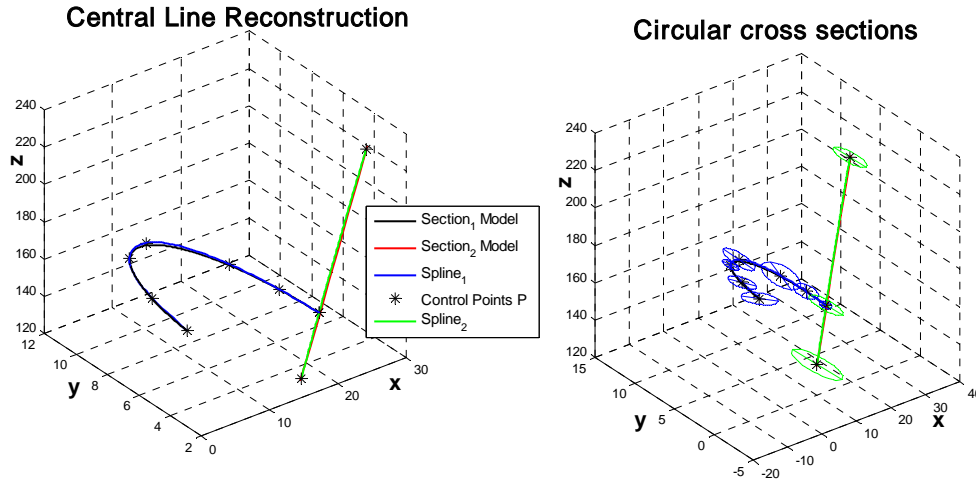


Figure 8. Reconstructed model; central lines (left) and circular cross-sections (right).

Applying the developed methodology and algorithm we obtain Figure 8, which portrays the reconstructed central line of the two segments of the model geometry. As we may observe, the reconstruction via the parametric spline of the model object is very good. In the same figure is also shown the result of creation of the circular cross-sections at selected sites of the object's central line.

3.3. Real case application

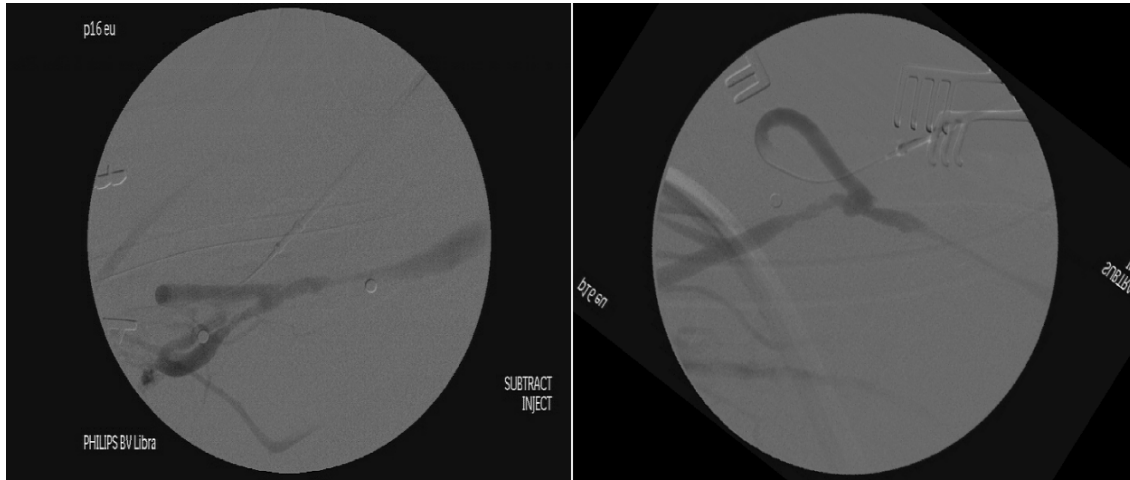


Figure 9. The selected angiography projections: On the left the 90° case is depicted while on the right the -20° one.

During the experiments, conducted at the Center of Experimental Surgery of the Foundation of Biomedical Research of the Academy of Athens as part of the 03ED 262 research project, various measurements were performed in a porcine model. In one such experiment, an angiography was performed at multiple angles with the aforementioned C-arm, Figure 9. The monitor output was recorded on DVD, which was later loaded into Info Cliper, a software developed by Canopus Co. Ltd.. This program was used to capture, in bmp format, the best images acquired at the various angles of interest. From these images, two were selected, based on image quality criteria, and are displayed in Figure 10.

4. CONCLUSIONS

In this study, we developed a methodology and the respective algorithm for determination of the 3D geometry of the central line of vessels from their biplane angiographic views. The method developed was based on the theory of C.E. Metz & L.E. Fencil^[1].

The relationship between the two systems of coordinates, i.e. the rigid rotational matrix and the translation vector, is unknown. However, due to the fact that this methodology is oriented to the specific problem described above, identification of this relationship amounts to calculation of the rotation angle and vertical displacement of the C-arm.

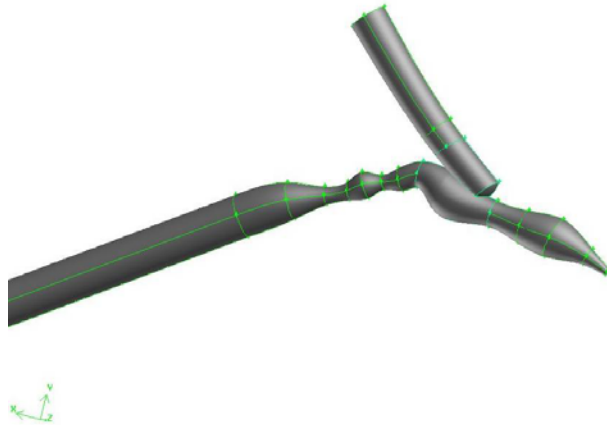


Figure 10. The reconstructed 3D geometry which was constructed in GAMBIT.

The image coordinates of two object points that can be defined unambiguously in both views are used to establish the relative geometry of the two projections. With these points, a 4×4 non-linear system is created with unknowns the angle and vertical displacement plus the z-coordinates of the points in space, which is solved using the Newton method for non-linear systems.

During simulations of 3D reconstruction through the developed methodology, we noticed that the non-linear system is extremely unstable and seems to have more than one roots. Consequently, accurate assessment of the image coordinates of the two points is very important. Provided that the geometry has been determined, we can proceed to the reconstruction of the object's central line. The epipolar line technique is employed to recognize respective object points in the two projections and for every pair of respective points the 3D coordinates of the real object point are estimated. The aforementioned process results in the acquisition of a set of 3D object points; this constitutes the control points for center line reconstruction using the parametric natural spline, whose parameter is the arc length. Advantages of the parametric spline approach are first that it facilitates the reconstruction of curves with steep changes and second that points not belonging to a function may be interpolated.

The method was tested using a model and showed that the accuracy of reconstruction depends on the number and quality of control points of the spline. One more distinguishing feature of the spline interpolation is that for the reconstruction of a curve there is a lower limit for the number of necessary control points, above which the accuracy of interpolation does not improve considerably.

Finally, the method was implemented on a model object with geometry analogous to that acquired from real angiographic views of arteriovenous anastomosis at the region of jugular vein, and its central line was reconstructed with very high accuracy.

ACKNOWLEDGEMENTS

This paper is part of the 03ED 262 research project, implemented within the framework of the "Reinforcement of Human Research Manpower" (PENED) and co-financed by National and Community Funds (25% from Greek Ministry of Development – General Secretariat of Research and Technology and 75% from E.U. – European Social Fund).

REFERENCES

- [1] C.E. Metz & L.E. Fencil, "Determination of three – dimensional structure in biplane radiography without prior knowledge of the relationship between the two views: Theory", Medical Physics 16, 1989, pp 45-51
- [2] K.R. Hoffmann, C.E. Metz, Y. Chen, "Determination of 3D imaging geometry & object configurations from two biplane views: an enhancement of the Metz – Fencil technique", Medical Physics 22, 1995, pp 1219-1227
- [3] S.Y.J. Chen & C.E. Metz, "Improved determination of biplane imaging geometry from two projection images & its application to 3D reconstruction of coronary arterial trees", Medical Physics 24, 1997, pp 633-654
- [4] K.R. Hoffmann et al, "A system for determination of 3D vessel tree centrelines from biplane images", International Journal of Cardiac Imaging 16, 2000, pp 315-330
- [5] K.R. Hoffmann et al, "3D reconstruction of the carotid artery from two views using a single centreline", International Congress Series 1268, 2004, pp 177-182
- [6] Manual of mobile C-arm, BV Libra, Philips Medical Systems